**ANU-P/1089**
**July 1991**

# SHAPE CO-EXISTENCE FROM THE STRUCTURE OF THE YRAST BAND IN $^{174}$Pt

**G.D. DRACOULIS, B. FABRICIUS, A.E. STUCHBERY**

*Department of Nuclear Physics, Research School of Physical Sciences and Engineering, Australian National University, GPO Box 4, Canberra ACT 2601, Australia*

**A.O. MACCHIAVELLI, W. KORTEN, F. AZAIEZ, E. RUBEL, M.A. DELEPLANQUE, R.M. DIAMOND AND F.S. STEPHENS**

ANU P/1089
Accepted for Publication in Rapid Communication in Physical Review C, July 1991

# SHAPE CO-EXISTENCE FROM THE STRUCTURE OF THE YRAST BAND IN $^{174}$Pt

G.D. DRACOULIS, B. FABRICIUS, A.E. STUCHBERY

*Department of Nuclear Physics, Research School of Physical Sciences and Engineering, Australian National University, PO Box 4, Canberra ACT 2601, Australia*

A.O. MACCHIAVELLI[1], W. KORTEN, F. AZAIEZ[2], E. RUBEL[3], M.A. DELEPLANQUE, R.M. DIAMOND and F.S. STEPHENS

*Nuclear Science Division, Lawrence Berkeley Laboratory, University of California, Berkeley CA 94720, USA*

*Abstract:* Excited states in the very neutron-deficient nucleus $^{174}$Pt have been identified up to spin 14. An irregular yrast sequence was observed beginning with a high $2^+ \rightarrow 0^+$ energy. It can be interpreted as the result of a change from a weakly-deformed ground state band, to a well-deformed rotor, near spin 6.

1 On leave from Comision Nacional de Energia Atomica, 1429 Buenos Aires, Argentina.
2 Permanent address: CEN-BG, IN2P3, Le Haut-Vigneau, 33170 Gradignan, France
3 Permanent address: University of California at Davis, California 95616, USA

Interference between collective bands based on competing nuclear shapes is accepted as the cause of irregularities at low spin in the yrast sequences of a number of nuclei, particularly at the boundaries of the deformed regions, approaching closed neutron or proton shells (see Ref. 1 for a review).

In mercury nuclei (Z=80), for which spectroscopic information now extends down to $^{180}Hg_{100}$ [2], the neutron-number dependence of the energy difference between the two collective band-heads (the lower one being poorly deformed, the higher one of well-deformed prolate character) shows a minimum near N=102. This feature is in broad agreement with theoretical expectations [3] since the minimum energy of the well-deformed configuration is expected near the middle of the N=82-126 neutron shell where interactions between valence protons and neutrons are maximised.

A further decrease in proton number (away from Z=82) leads into the region where the nuclei could already be well-deformed in the ground state. Hence both the difference in deformation between competing minima in the nuclear potential well and the height of the potential barrier between them should decrease. Less pronounced perturbations could therefore be expected, specifically because the differences in moments-of-inertia will be smaller and the band interactions, larger.

Thus, while the lightest platinum case previously reported, $^{176}_{78}Pt_{98}$, shows effects interpreted as shape co-existence at low spin [4,5], only small perturbations are evident in the heavier (A≥178) isotopes. In those, the more deformed well is proposed [4-6] to be the lower while $^{176}Pt$ is the first of the isotopes (with decreasing N) in which the ground state belongs to the less-deformed well. Since the ground state of $^{174}Pt_{96}$ is likely to be even less-deformed, and if the well-deformed ("intruder") band occurs at a relatively higher excitation energy, a pronounced anomaly can be anticipated.

This letter reports the first spectroscopic results for $^{174}Pt$. It was populated using the $^{107}Ag$ ($^{70}Ge$,p2n)$^{174}Pt$ reaction with $^{70}Ge$ beams from the Lawrence Berkeley Laboratory (LBL), 88 Inch Cyclotron following studies at the ANU 14UD Pelletron with the same reaction and also with the $^{144}Sm$ ($^{33}S$,3n)$^{174}Pt$ reaction.

Because of its neutron deficiency, the population of $^{174}$Pt will be efficient only through reactions involving proton emission. Fission competition is an irreducible limiting factor. For the $^{107}$Ag + $^{70}$Ge combination, (compound nucleus $^{177}$Au), chosen on the basis of statistical model cross-section calculations (with treatment of the heavy-ion fusion near the Coulomb barrier using the prescriptions of Esbensen [7]), fission was expected to dominate but with practicable cross-section remaining in the evaporation residue channels. The energy chosen for the main measurements was 303 MeV, so that with a target of 0.9mg/cm$^2$ an energy integration from 303 to 286 MeV is effected, covering the region of 3-particle evaporation, leading mainly to $^{174}$Pt and $^{174}$Ir.

Gamma-rays were detected in the LBL array HERA which consists of 20 Compton-suppressed Ge spectrometers and a 40-element BGO central ball. The 0.9 mg/cm$^2$ target was sufficiently thin to allow recoiling nuclei to decay in flight, so that residues could be confirmed by their Doppler shifts. Approximately $4 \times 10^8$ $\gamma$-$\gamma$ coincidence events were collected with the requirement that two or more additional $\gamma$-rays were detected in both halves of the BGO ball. This substantially reduced the intensity of lines from Coulomb excitation of the target. Coincidence spectra for individual $\gamma$-rays were generated from 2-dimensional matrices constructed for dual combinations of all detectors as well as with the detectors grouped in related angles, allowing the evaluation of $\gamma$-$\gamma$ correlations [8].

Except for $^{174}$Pt and $^{174}$Ir, populated by the two most prolific channels (2np and n2p respectively) all other expected products, listed in table 1, have been studied previously by $\gamma$-ray spectroscopy, including $^{175}$Pt [9], the only other *platinum* isotope expected. The predicted products were observed with relative proportions in encouraging agreement with the calculations (given the known uncertainties), as shown in table 1.

Two other $\gamma$-$\gamma$ coincidence experiments were carried out with the ANU 14UD Pelletron accelerator and the 6-detector array, CAESAR. The first used the same $^{107}$Ag target and a lower $^{70}$Ge beam energy of 290 MeV. The second was with an alternative reaction using 153 MeV $^{33}$S incident on a 3.0 mg/cm$^2$ $^{144}$Sm target (at 45° to the beam axis and backed with a lead layer to stop recoils) in which the main products following particle evaporation from the compound nucleus $^{177}$Pt were expected to be $^{174}$Ir (2np) and $^{174}$Os (n2p). In this case, only a minor channel (3n) would lead to $^{174}$Pt. The transitions assigned to $^{174}$Ir and $^{174}$Pt in the $^{70}$Ge induced reaction were again observed, with the appropriate difference in relative intensity.

A combined spectrum from the LBL measurement with gates set on the main $\gamma$-rays at 394, 462, 473, 498 and 532 keV assigned to $^{174}$Pt is shown in fig. 1. All are in mutual coincidence and also in cascade with lines at 551 and 570. These and several other transitions assigned to the level scheme are shown in table 2, together with relative intensities. Platinum X-rays are observed clearly in coincidence with these transitions allowing a definitive assignment to $^{174}$Pt (since they do not belong to $^{175}$Pt). Several of the gates and particularly the 394 keV line have minor contamination from known osmium isotopes (as indicated in fig. 1) whose proportion varies in the different cross-bombardments. The separation between iridium and platinum X-rays is shown in fig. 2 which overlays coincidence spectra from gates on known iridium lines and the group of lines assigned to $^{174}$Pt.

The ordering of transitions in the yrast cascade indicated in fig. 1 is both by intensity above the 394 and 498 keV pair and also by the observation of transitions at 431 and 885 keV which feed in at different levels in the main cascade as shown in the level scheme in fig. 3. The 394 and 498 keV lines are too close in intensity (after correction for internal conversion) to be ordered unambiguously, although the suggested order (with the 394 keV line as the $2^+ \rightarrow 0^+$ transition) is marginally favoured and also supported by a tentative 882 keV line which feeds the 394 keV transition but not the 498 keV line.

The rapid drop in intensity with spin is consistent with the anticipated depletion of high input $\ell$-values by the strong fission channel. The difficulty in observing higher states is exacerbated by the Doppler broadening which becomes significant at high energy although this is not a resolution limitation in the $^{33}$S induced reaction.

Spectroscopic information is limited to anisotropies for the 394, 461, 473 and 497 keV lines, which support a stretched quadrupole character and the $\gamma$-$\gamma$ correlation information (DCO) which confirms a sequence of stretched quadrupoles up to the 551 keV transition, as shown in Table 1(b). (Statistical accuracy was insufficient to define the higher transitions.)

The major irregularity in the yrast level scheme implied in fig. 1 is apparent from a comparison of alignments for the yrast bands of $^{174}$Pt, $^{176}$Pt and $^{178}$Pt shown in fig. 3. The irregular structure† can be interpreted as the result of a crossing between a poorly-deformed ground-state sequence and a more-deformed excited band with a moment-of-inertia similar to that in $^{176}$Pt above spin 6. The unperturbed bands required to reproduce experiment in a band-mixing calculation (details of which will be published elsewhere) have moments-of-inertia which, when related to quadrupole moments, agree both with the scenario presented in the introduction and, in detail, with the systematics of uncoupled ground and intruder bands published recently [10]. That the mixing matrix element of 82 keV required is comparable to that used in band-mixing for $^{180}$Hg [2], and contrasts with the larger value (160 keV) used [4] for $^{176}$Pt, is also in agreement with a clearer separation between the potential minima.

From the calculations, an excited $0^+$ state would be expected at 710 keV (corresponding to the perturbed 'intruder' band-head). When this calculated state and the observed yrast states are included in the systematics for the platinum isotopes, a distinctive symmetry about N=103 is apparent (fig. 4), similar to that observed in the mercury isotopes and perhaps significantly lower than the midshell (by simple counting) of N=104. Explanation of this systematic would be a suitable target for collective theories which are sensitive to the role of proton-neutron interactions across a shell.

Total Routhian surface (TRS) calculations which estimate the nuclear potential energy as a function of rotational frequency predict [9,11] a very gamma-soft ground state in $^{174}$Pt with $\beta_2 \simeq 0.13$ and $\gamma = -25°$ and also a shape change to $\beta_2 \simeq 0.21$, $\gamma = +9°$ near $\hbar\omega = 0.22$ MeV. The shape change however, is associated with, and stabilised by, the rotational *alignment* of $i_{13/2}$ neutrons. In other words, the crossing band is not simply one of larger quadrupole deformation. This prediction is similar to that proposed by Cederwall et al. [9] in their interpretation of the yrast scheme of $^{176}$Pt. However, although one cannot expect

---

† The alternative ordering of the 394 and 498 keV transitions would lead to even more irregularity.

detailed agreement between such calculations and experiment, it is the case that those calculations lead to a more complicated alignment trajectory at low spin than is observed experimentally (see figure 8 of Ref. 9). The distinction between this mechanism of simultaneous alignment and shape change and one where a shape change is caused by a spin zero-coupled $h_{9/2}$ proton-pair excitation, as proposed [3] for the mercury isotopes and inferred [3,4] for the light platinum isotopes is worthy of consideration.

**Acknowledgements**

We acknowledge the contributions of A.P. Byrne and T. Kibèdi who participated in the ANU measurements, the staff of the ANU 14UD Pelletron facility for their support and the staff of the 88 Inch Cyclotron at LBL for their efforts. We are grateful to W. Nazarewicz and R. Wyss who kindly provided calculations prior to publication and for discussions. G.D.D., A.E.S. and B.F. received support under the DITAC program for access to major overseas research facilities.

**References**

1 J.H. Hamilton in Treatise on Heavy-Ion Science Vol. 8, p1. (Edited by D. Allan Bromley) Plenum Publishing Corporation (1989).

2 G.D. Dracoulis, A.E. Stuchbery, A.O. Macchiavelli, C.W. Beausang, J. Burde, M.-A. Deleplanque, R.M. Diamond and F.S. Stephens, Phys. Lett. 208 (1988) 365.

3 R. Bengtsson, T. Bengtsson, J. Dudek, G. Leander, W. Nazarewicz and J.-Y. Zhang, Phys. Lett. B 183 (1987) 1.

4 G.D. Dracoulis, A.E. Stuchbery, A.P. Byrne, A.R. Poletti, S.J. Poletti, J. Gerl and R.A. Bark, J. Phys. G 12 (1986) L97.

5 R. Bengtsson, J.-Y. Zhang, J.H. Hamilton and L.K. Peker, J. PHys. G: Nucl Phys 12 (1986) L223.

6 G.D. Dracoulis, B. Fabricius, R.A. Bark, A.E. Stuchbery, D.G. Popescu and T. Kibèdi, Nucl. Phys. A 510 (1990) 533.

7 H. Esbensen, Nucl. Phys. A 352 (1981) 147.

8 F.S. Stephens, Proc. Niels Bohr Centennial Conf. (Copenhagen, 1985) eds. R. Broglia, G. Hagemann and B. Herskind (North-Holland, Amsterdam, 1985) p363.

9 B. Cederwall et al., Z. Phys. A 337 (1990) 283.

10 B.R. Barrett, G.D. Dracoulis and R.A. Bark, Phys. Rev. C43 (1991) R926.

11 W. Nazarewicz and R. Wyss, private communication.

**Table 1**
**Observed evaporation residues**

| Nuclide | Evaporation Channel | Proportion Observed [a] | Calculated [b] |
|---|---|---|---|
| $^{168}W$ | p2α | 2 | 4 |
| $^{171}Re$ | 2pα | 6 | 7 |
| $^{171}Os$ | pnα | 11 | 16 |
| $^{172}Os$ | pα | 7 | 4 |
| $^{173}Os$ | n3p | 1 | 3 |
| $^{174}Os$ | 3p | 6 | 5 |
| $^{173}Ir$ | 2n2p | 3 | |
| $^{174}Ir$ | n2p | 25 [c] | 23 |
| $^{175}Ir$ | 2p | 6 | 1 |
| $^{174}Pt$ | 2np | 25 | 26 |
| $^{175}Pt$ | np | 12 | 5 |

a) Approximate yield deduced from coincidence γ-rays

b) Statistical model calculation with Esbensen [7] treatment of fusion near the barrier and integration from 286 to 303 MeV

c) assumed since the level scheme is unknown

**Table 2**
**Gamma-rays assigned to $^{174}Pt$**

| Energy (keV) | Relative Intensity | Assignment $J_i$ $J_f$ | DCO ratios |
|---|---|---|---|
| 394.2 | 100 | $2^+ \rightarrow 0^+$ | 0.96 (14) |
| 497.6 | 103 (5) | $4^+ \rightarrow 2^+$ | 0.91 (9) |
| 473.2 | 93 (5) | $6^+ \rightarrow 4^+$ | 1.04 (15) |
| 461.6 | 75 (4) | $8^+ \rightarrow 6^+$ | 0.95 (8) |
| 501.5 | 42 (3) | $10^+ \rightarrow 8^+$ | 0.91 (12) |
| 551.1 | 30 (2) | $12^+ \rightarrow 10^+$ | 1.17 (13) |
| 569.9 | 18 (2) | $14^+ \rightarrow 12^+$ | |
| 284.0 | 8 (1) | | |
| 431.1 | 18 (2) | $(7) \rightarrow 6^+$ | 0.58 (20) |
| (882) | 8 (2) | $2^+$ | |
| 885 | 13 (2) | $4^+$ | |

## Figure Captions

Fig. 1 Combined coincidence spectrum with gates on the main yrast transitions assigned to $^{174}Pt$. Connecting lines indicate the proposed ordering.

Fig. 2 Comparison between the low-energy region of the spectrum with gates set on transitions in iridium products and the gates of fig. 1.

Fig. 3 Aligned angular momenta (approximately equal to I-1/2 where I is the spin of the decaying state) versus rotational frequency for yrast bands in light platinum isotopes. (Results for $^{176}Pt$ and $^{178}Pt$ from Ref. 4 .

Fig. 4 Yrast positive parity states and excited $0^+$ states (observed – filled squares; predicted from 2-band fit – open square) in even platinum isotopes.

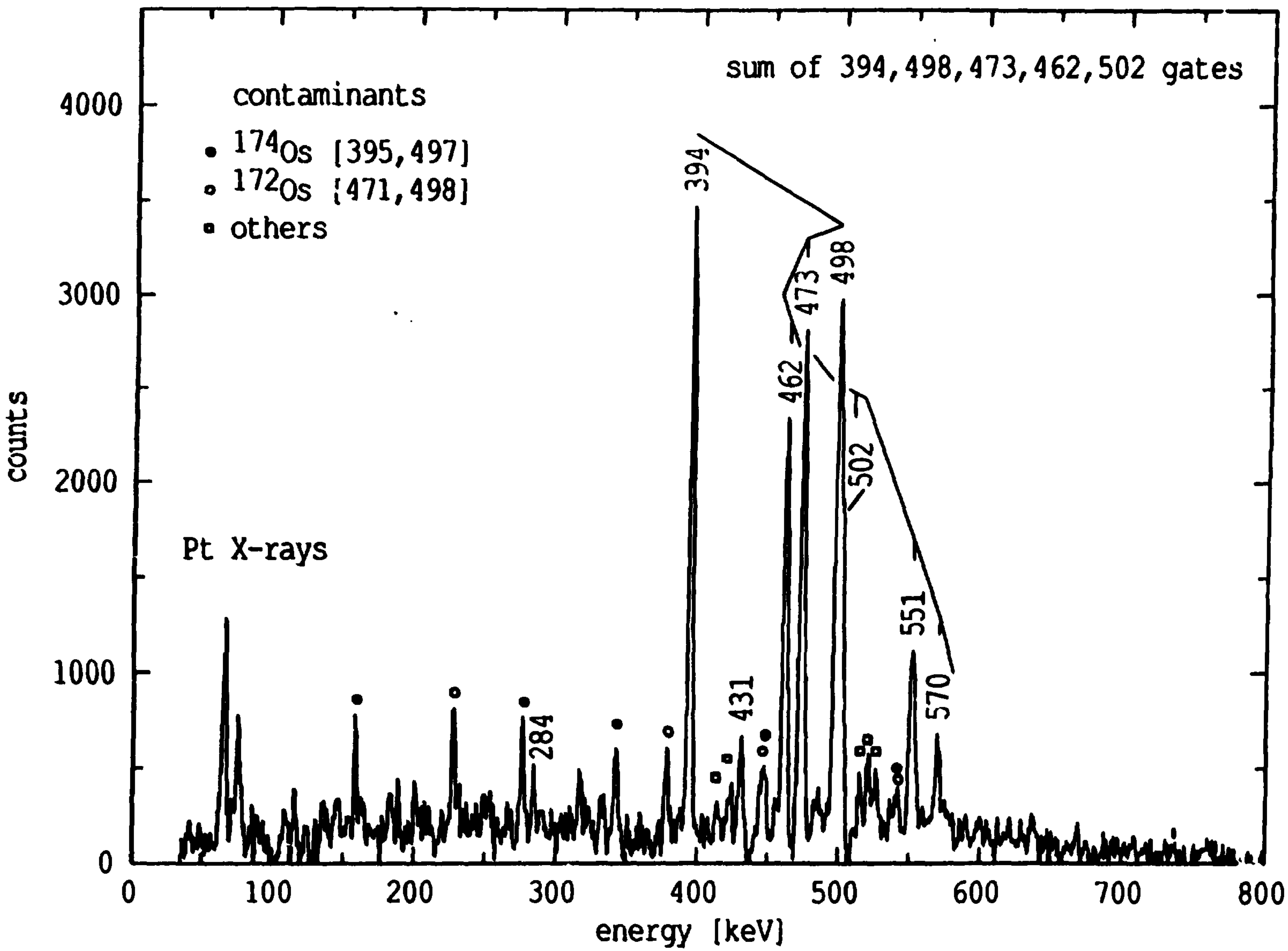
sum of 394,498,473,462,502 gates
contaminants
174Os [395,497]
172Os [471,498]
others
Pt X-rays
394
462
473
498
502
551
570
431
284
counts
energy [keV]
0
1000
2000
3000
4000
0
100
200
300
400
500
600
700
800

figure 1

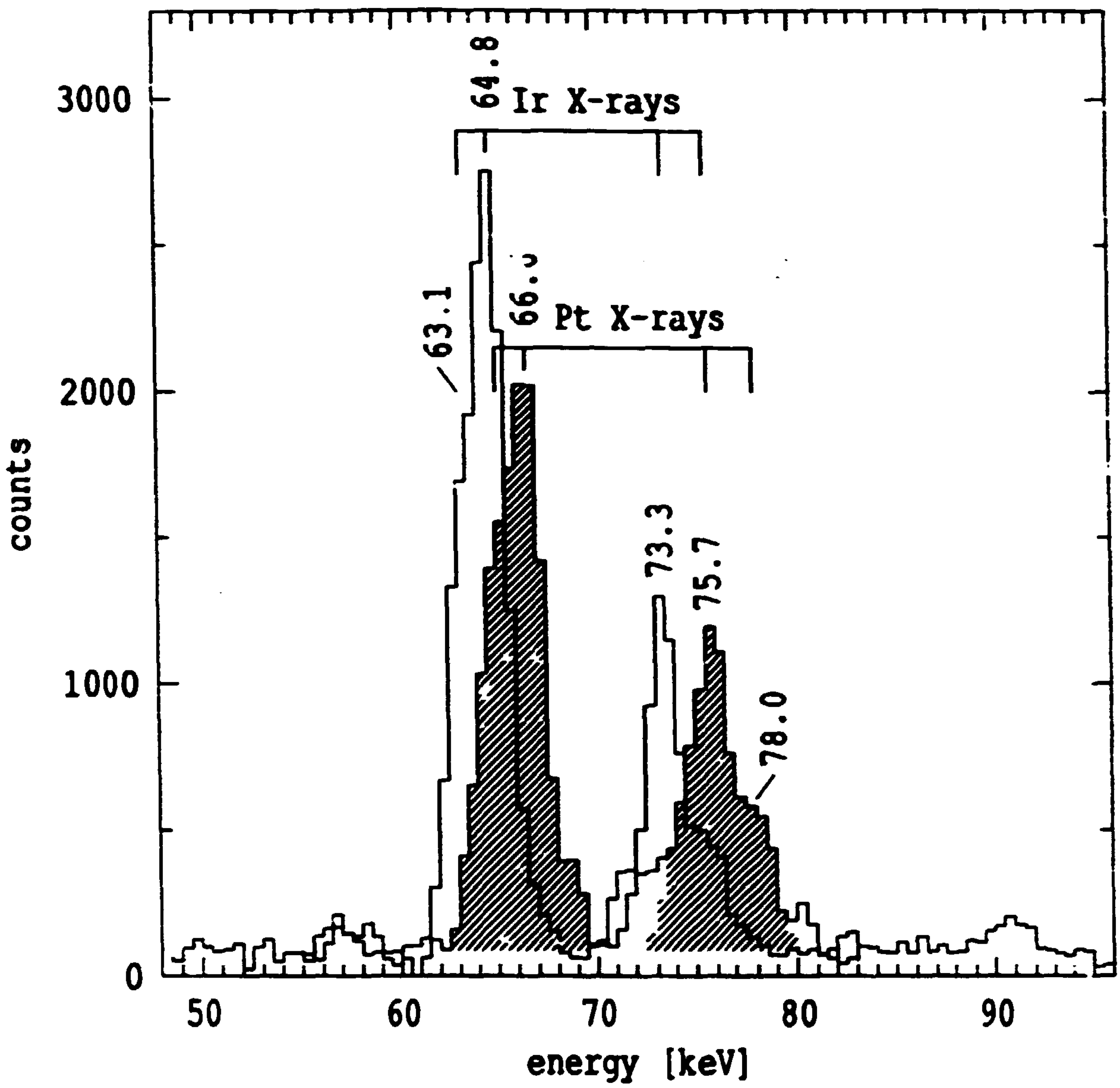

3000
2000
1000
0
counts
50
60
70
80
90
energy [keV]
64.8
Ir X-rays
63.1
Pt X-rays
73.3
75.7
78.0


*figure 2*

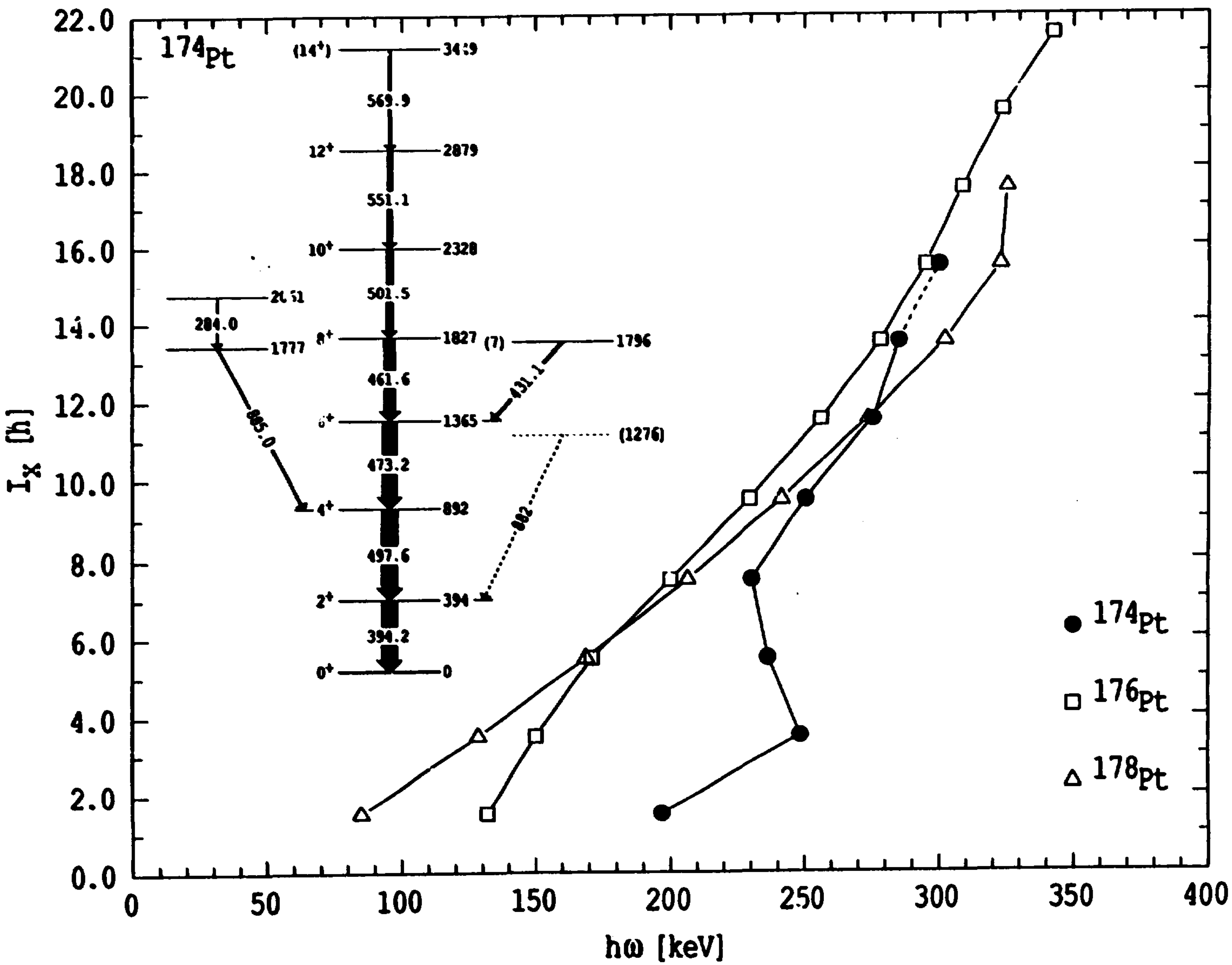

174Pt
(14+)
3419
569.9
12+
2879
551.1
10+
2328
501.5
8+
1827
461.6
1365
473.2
4+
892
497.6
2+
394
394.2
0+
0
284.0
1777
885.0
(7)
1796
431.1
(1276)
882
● 174Pt
□ 176Pt
△ 178Pt
Ix [ħ]
hω [keV]
22.0
20.0
18.0
16.0
14.0
12.0
10.0
8.0
6.0
4.0
2.0
0.0
0
50
100
150
200
250
300
350
400


figure 3

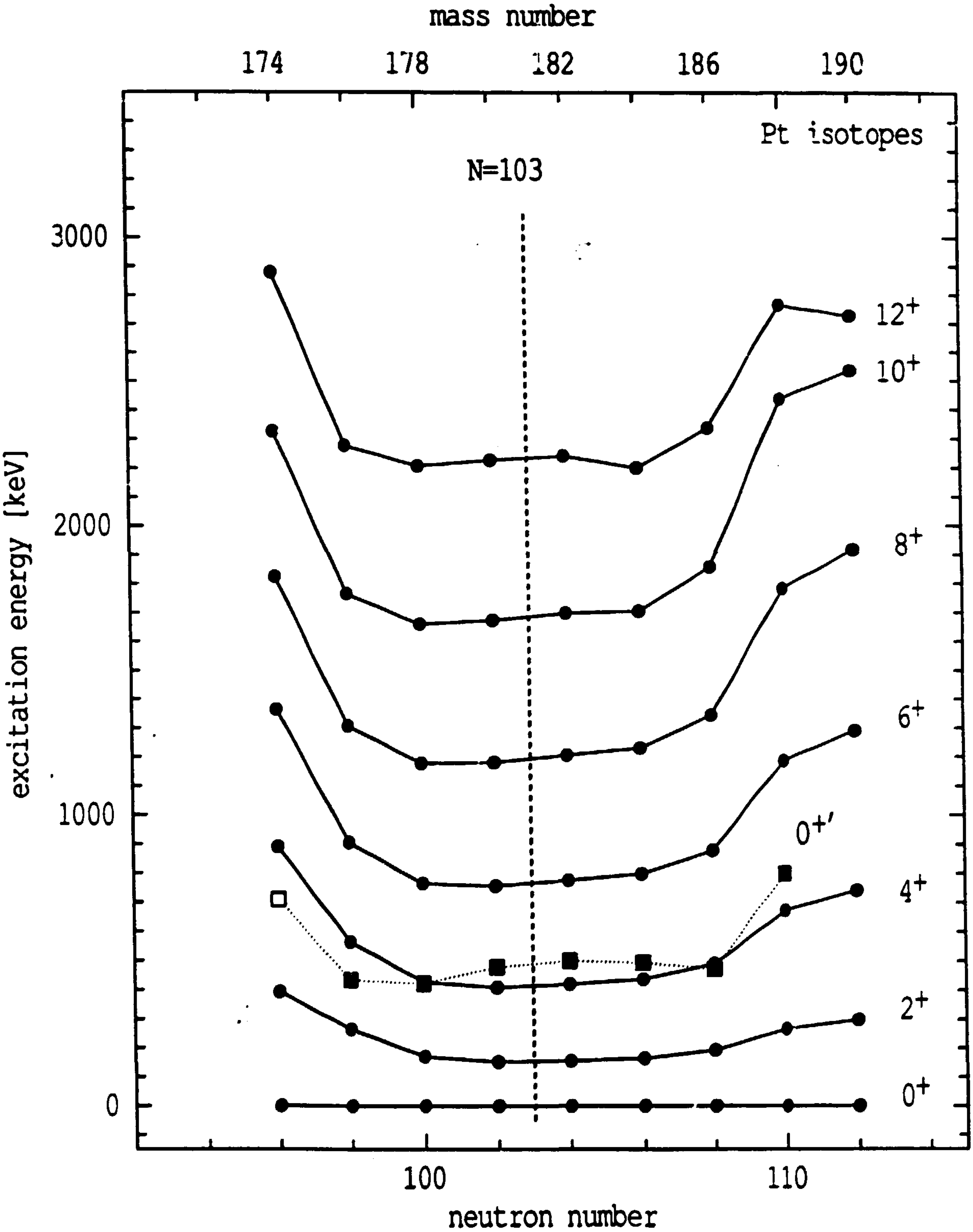

mass number
174
178
182
186
190
Pt isotopes
N=103
3000
2000
1000
0
12+
10+
8+
6+
0+'
4+
2+
0+
excitation energy [keV]
100
110
neutron number


figure 4